

Matter density distribution of GRMHD jets driven by black holes

Taiki OGIHARA (Tohoku Univ.)

Takumi OGAWA (Tsukuba Univ.)

Kenji TOMA (Tohoku Univ.)

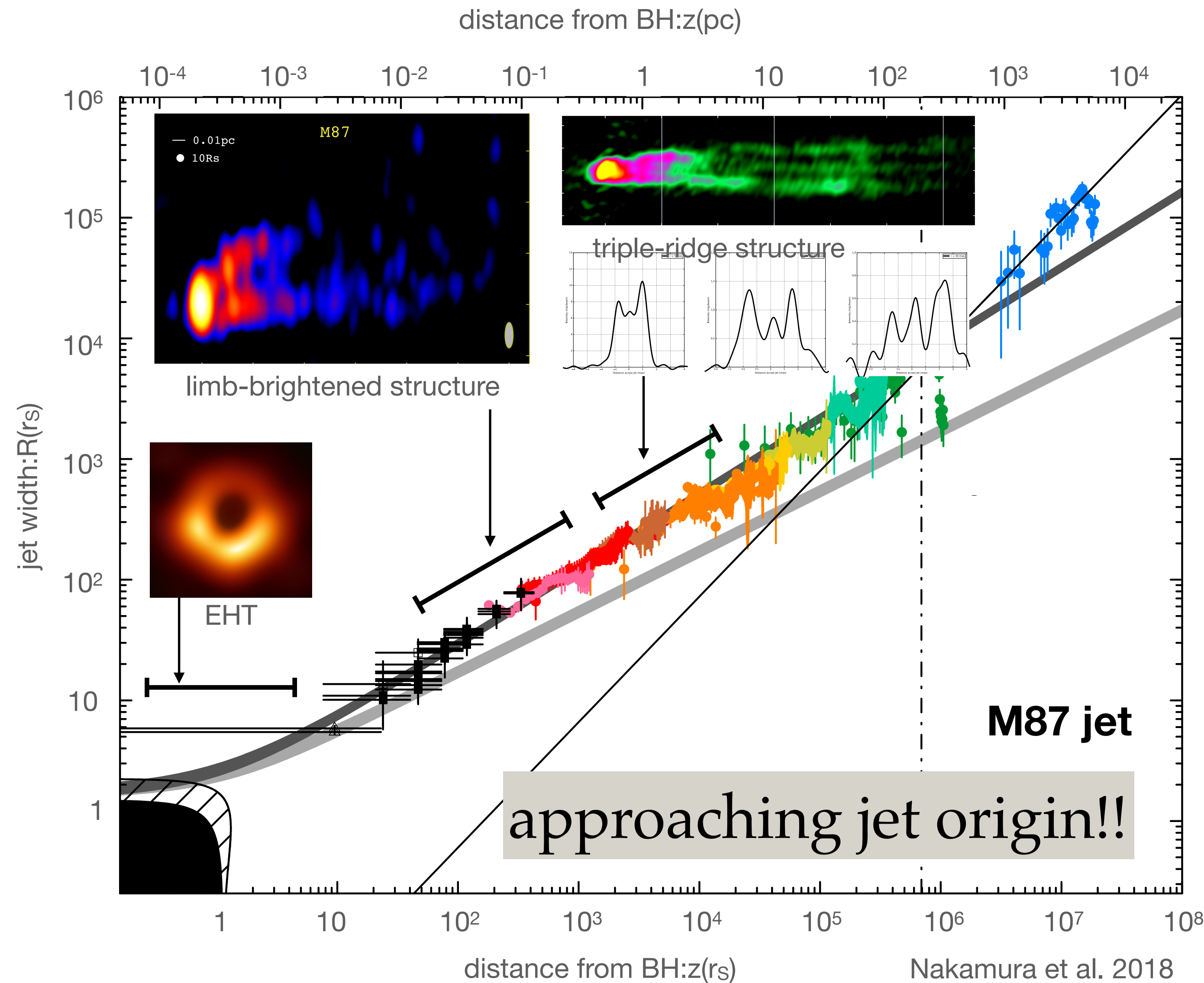
Black Hole Astrophysics with VLBI, 2021/January/18, online



Radio observations

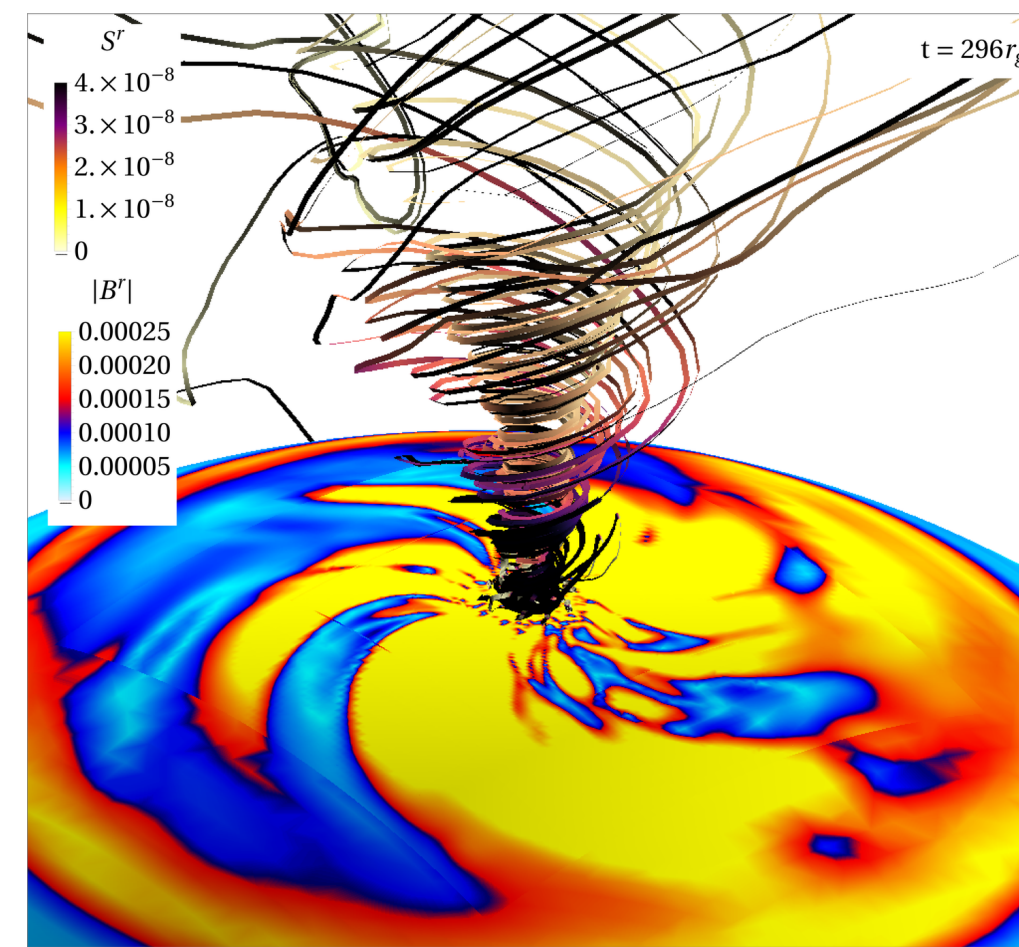
The jet origin is near the BH.

- High-resolution VLBI observations have resolved jets and revealed detailed emission structures.
- limb-brightened: M87, Mrk 501, Mrk 421, Cyg A, 3C84
- triple-ridge: only in high-sensitivity observation of M87
- jet width profile
- Jet emission near the horizon is not observed yet.

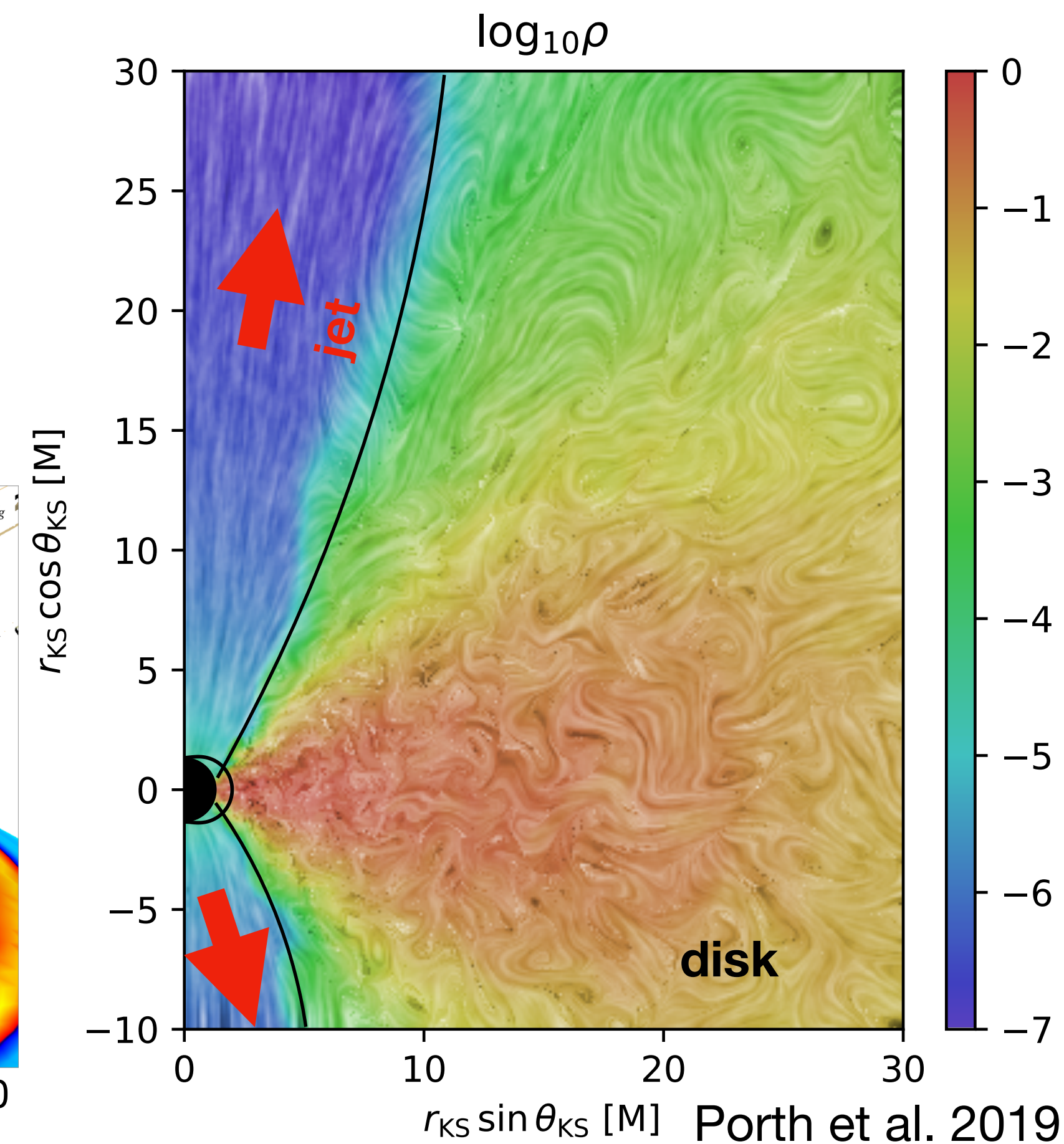


GRMHD simulations comparison to observations

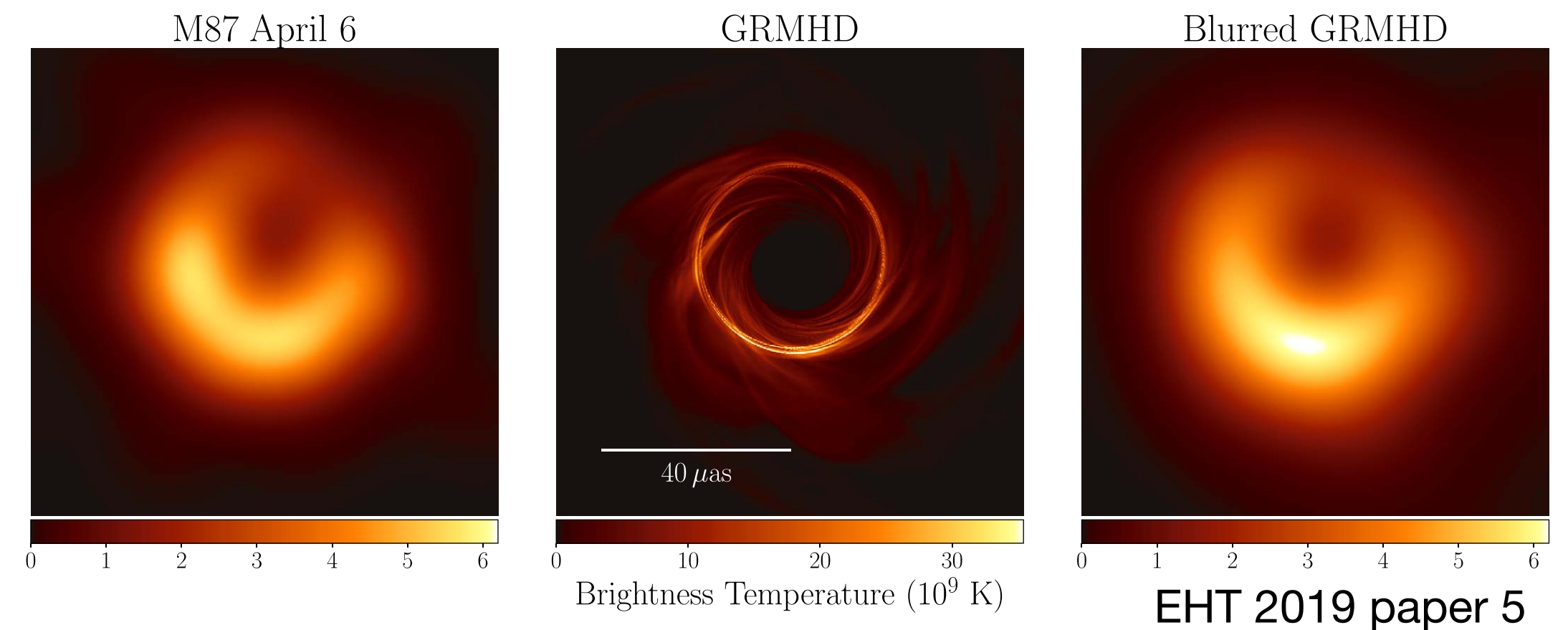
- The plausible jet launching mechanism is the Blandford-Znajek process.
 - rotational energy of BH
 - Poynting flux
 - kinetic energy
- GRMHD simulations supports the BZ process.
- Combining with radiative transfer calculations, one can create synthetic images.
 - compare theoretical models with observations = “black hole shadow”



Mahlmann, Levinson, Aloy 2020



Porth et al. 2019



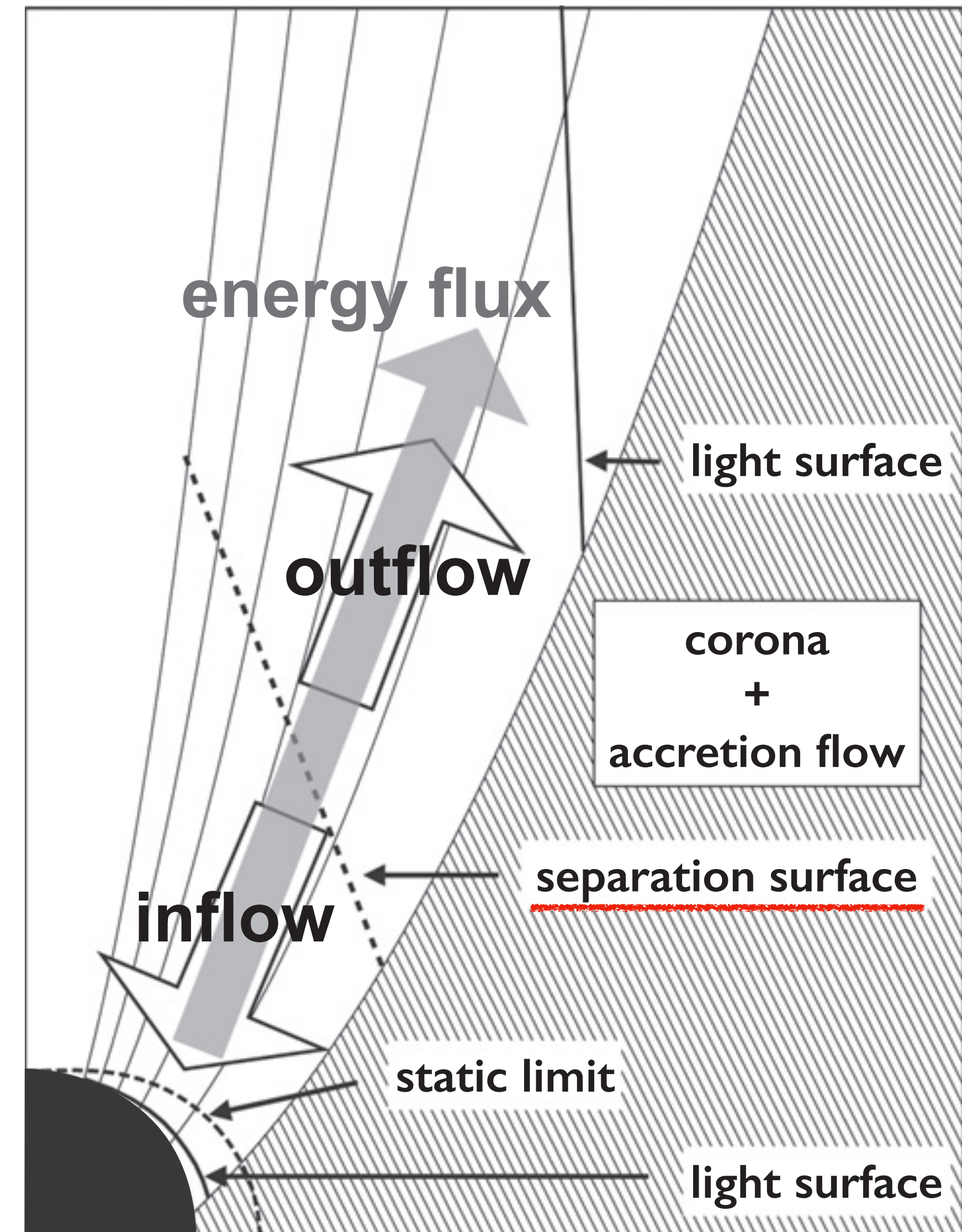
Brightness Temperature (10^9 K)

EHT 2019 paper 5

Density-floor in GRMHD simulations

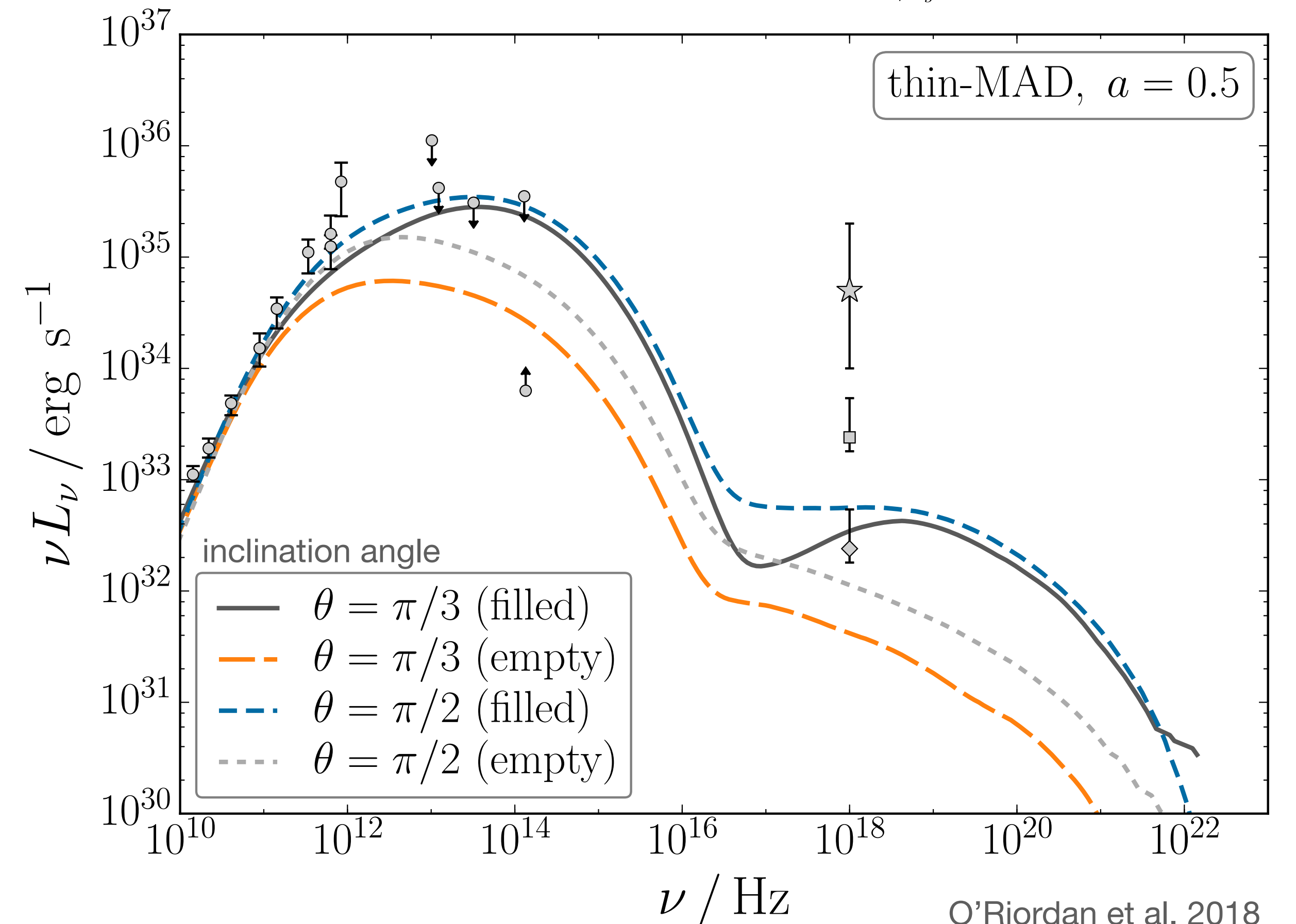
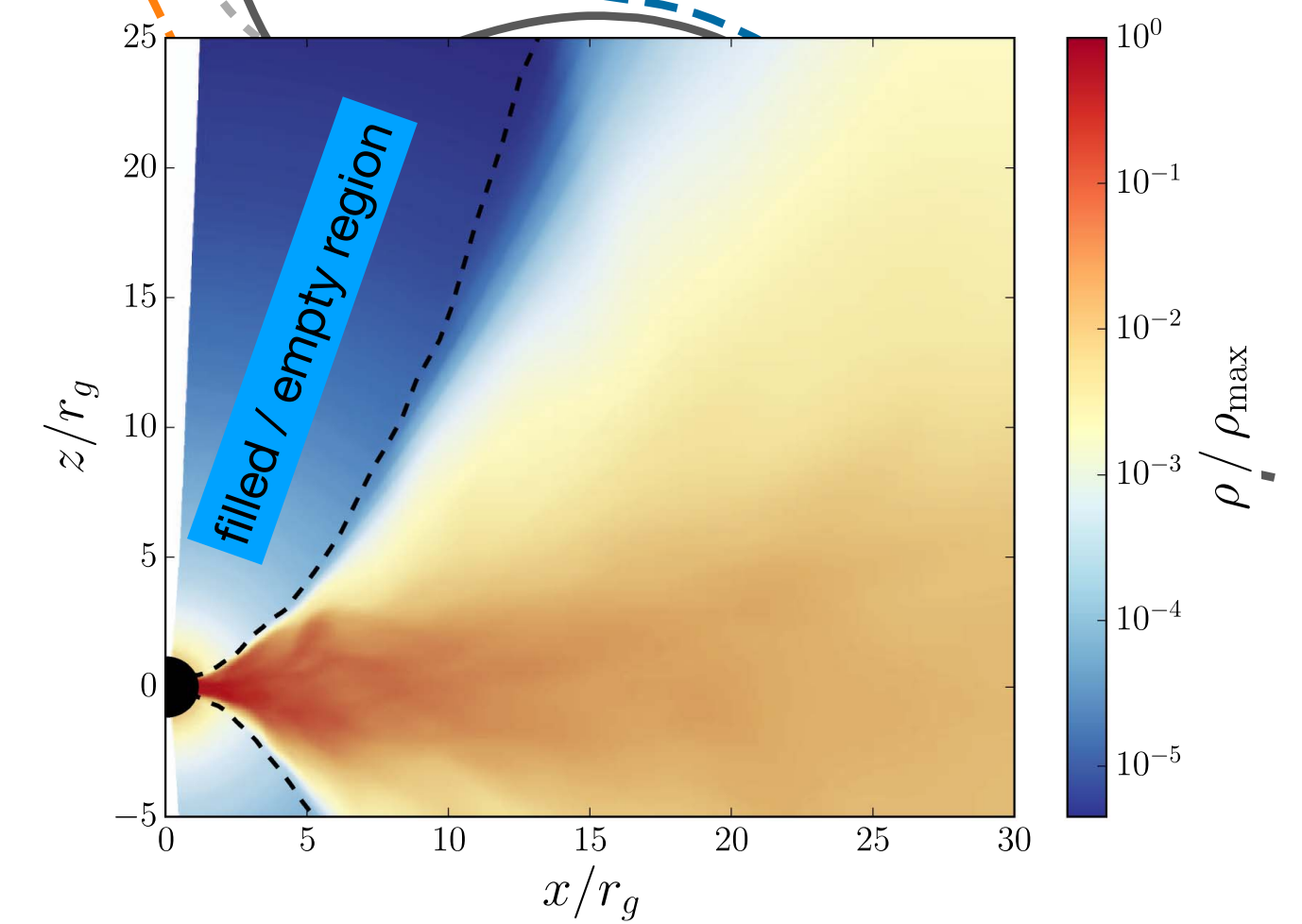
- Thermal plasma cannot dissipate into the highly magnetized region.
- In GRMHD simulations, the separation surface between the inflow and outflow emerges at the balanced surface of the gravity and the Lorentz force.
- **Density becomes very low in the jet.** Due to the numerical difficulty, density is replaced by “floor values” in simulations.

e.g., $\rho_{0,min} = 10^{-4} r^{-3/2}$, $u_{min} = 10^{-6} r^{-5/2}$
(McKinney & Gammie 2004)



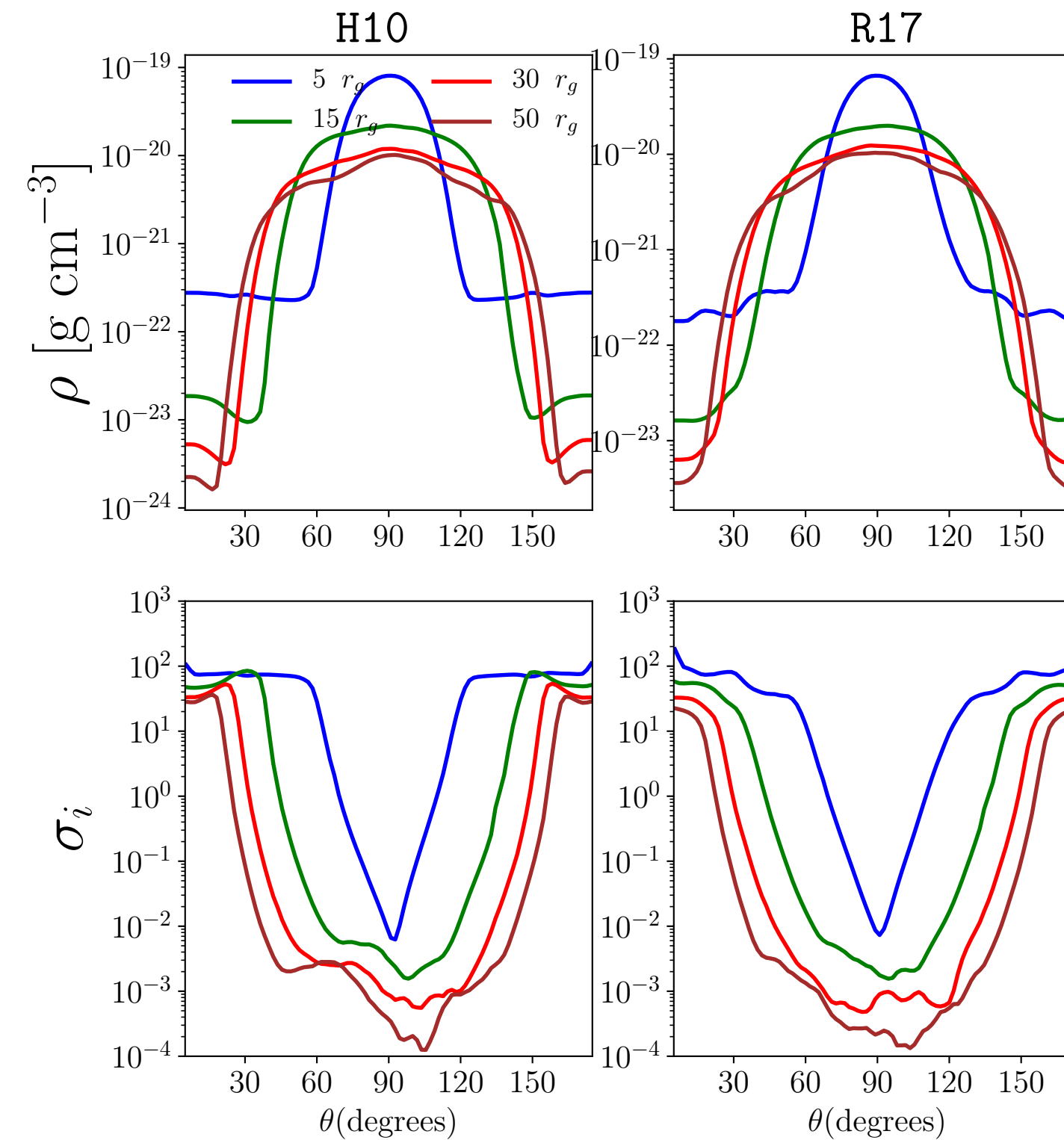
Density-floor effect on observations

- O’Riordan et al. 2018
 - 3D GRMHD simulation
 - calculate spectra for Sgr A*
 - filled / empty highly-magnetized funnel region
 - radio spectrum do not change significantly because the emission comes from the funnel edge.
 - IR and optical flux are enhanced in the filled case relative to the empty funnel case.

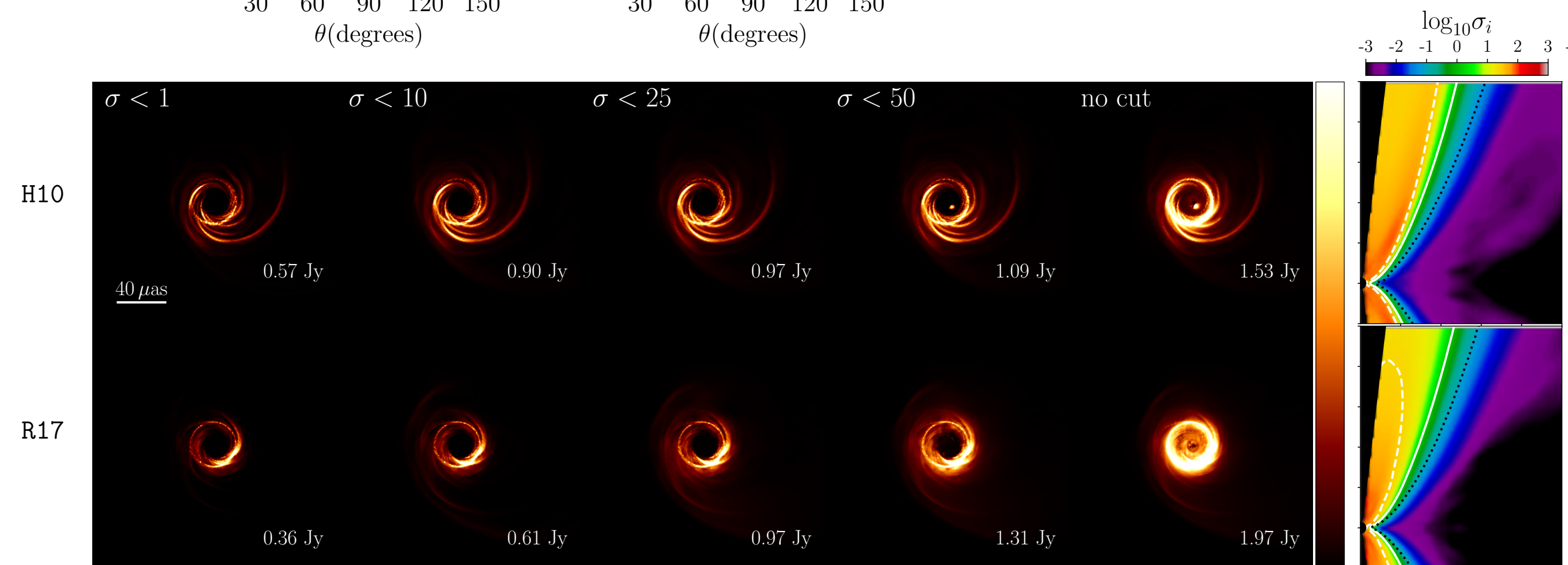


Density-floor effect on observations

- Chael et al. 2019
 - 3D GRMHD simulation
 - ignore a region $\sigma > \sigma_{\text{cut}}$ when calculate radiative transfer
 - no σ cut model: spectrum change at $\nu \gtrsim 230$ GHz
 - brighter ring/jet
- **The emission from the funnel region is not explored much.**



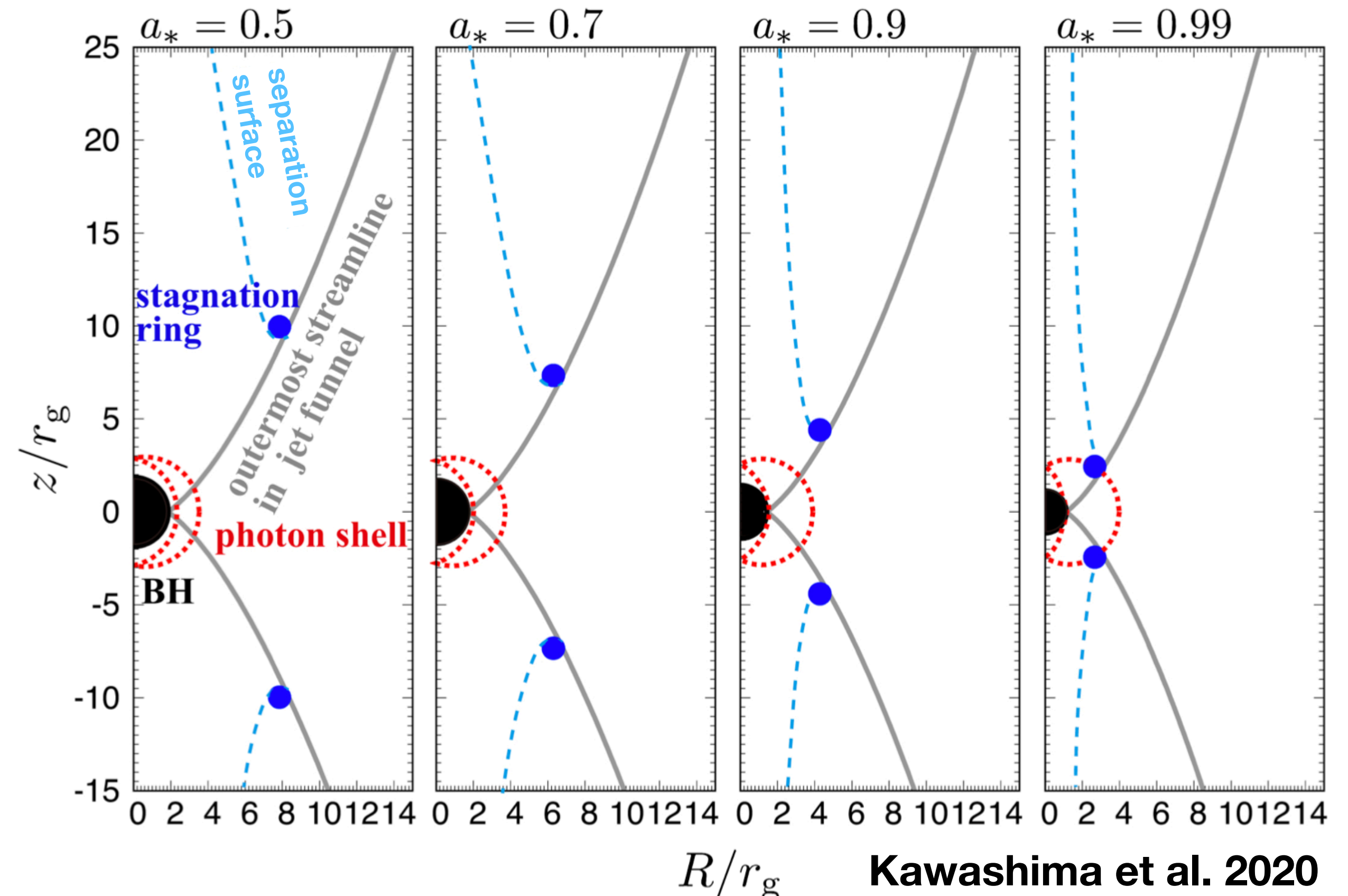
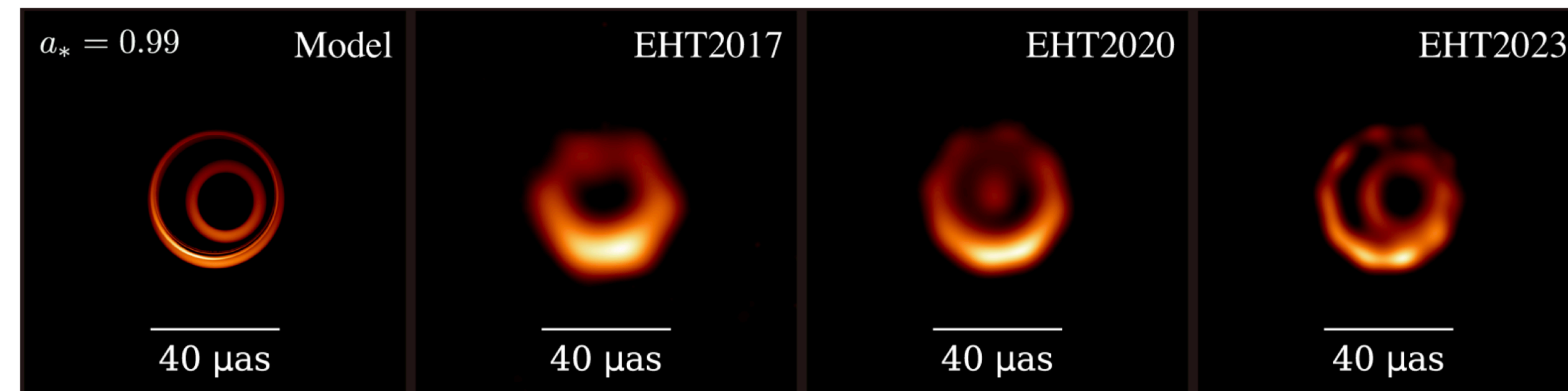
The density reaches the floor-value in the polar region where ρ and σ_i become flat.



Emission from Jet Origin

EHT scale observation

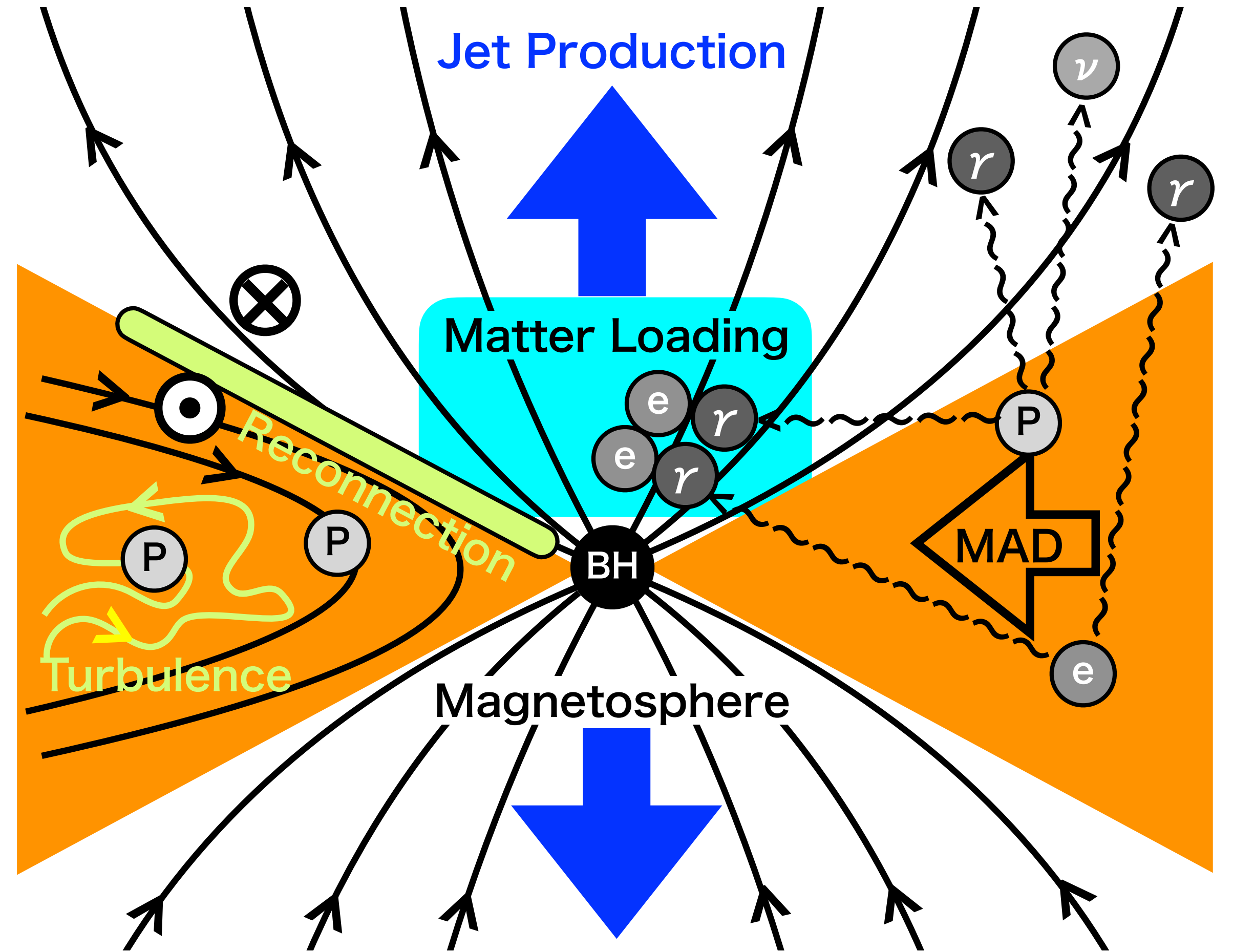
- Kawashima et al. 2020
 - radiative transfer calculation of the emission from the separation surface
 - reproduce the ring structure of EHT observation in 2017
 - In future observations, additional ring may be seen.
- **Emission from the jet may also be important to interpret the future EHT observations.**



Injection Mechanisms

not conclusive

- steady jets require an injection mechanism
 - pair-creation in jet?
(Levinson & Rieger 2011, Kimura & Toma 2020)
 - pair cascade?
(Broderick & Tchekhovskoy 2015, Kisaka+2020)
 - reconnection at jet edge?
(Dexter+14, Parfrey+15, Nathanail+20)
 - decay of relativistic non-charged particles?
(Toma & Takahara 2012)
- **uncertainty of the density distribution inside the jet**
→ **uncertainty of the synthetic images**



Kimura & Toma 2020

Our Motivation

predict jet images in EHT scale

- Focus on the internal structures of jets
- Construct **a semi-analytic model which do not suffer from the density floor problem**
- Determine the density distribution in a jet near the black hole
- In future, our jet model combined with radiative transfer calculations predicts/reproduce observed jet images

2. steady, axisymmetric, GRMHD jet model

Basic Equations

- basic equations

Maxwell equation:

$$\nabla_{\nu} F^{\mu\nu} = J^{\mu}, \quad \nabla_{\nu} * F^{\mu\nu} = 0$$

Energy-momentum equation:

$$\nabla_{\nu} T^{\mu\nu} = 0,$$

$$T^{\mu\nu} = \rho u^{\mu} u^{\nu} + \frac{1}{4\pi} \left(F^{\mu\lambda} F_{\lambda}^{\nu} - \frac{1}{4} g^{\mu\nu} F^{\lambda\sigma} F_{\lambda\sigma} \right)$$

$$\text{continuity equation: } (n u^{\mu})_{;\mu} = 0$$

$$\text{ideal MHD condition: } u^{\nu} F_{\mu\nu} = 0$$

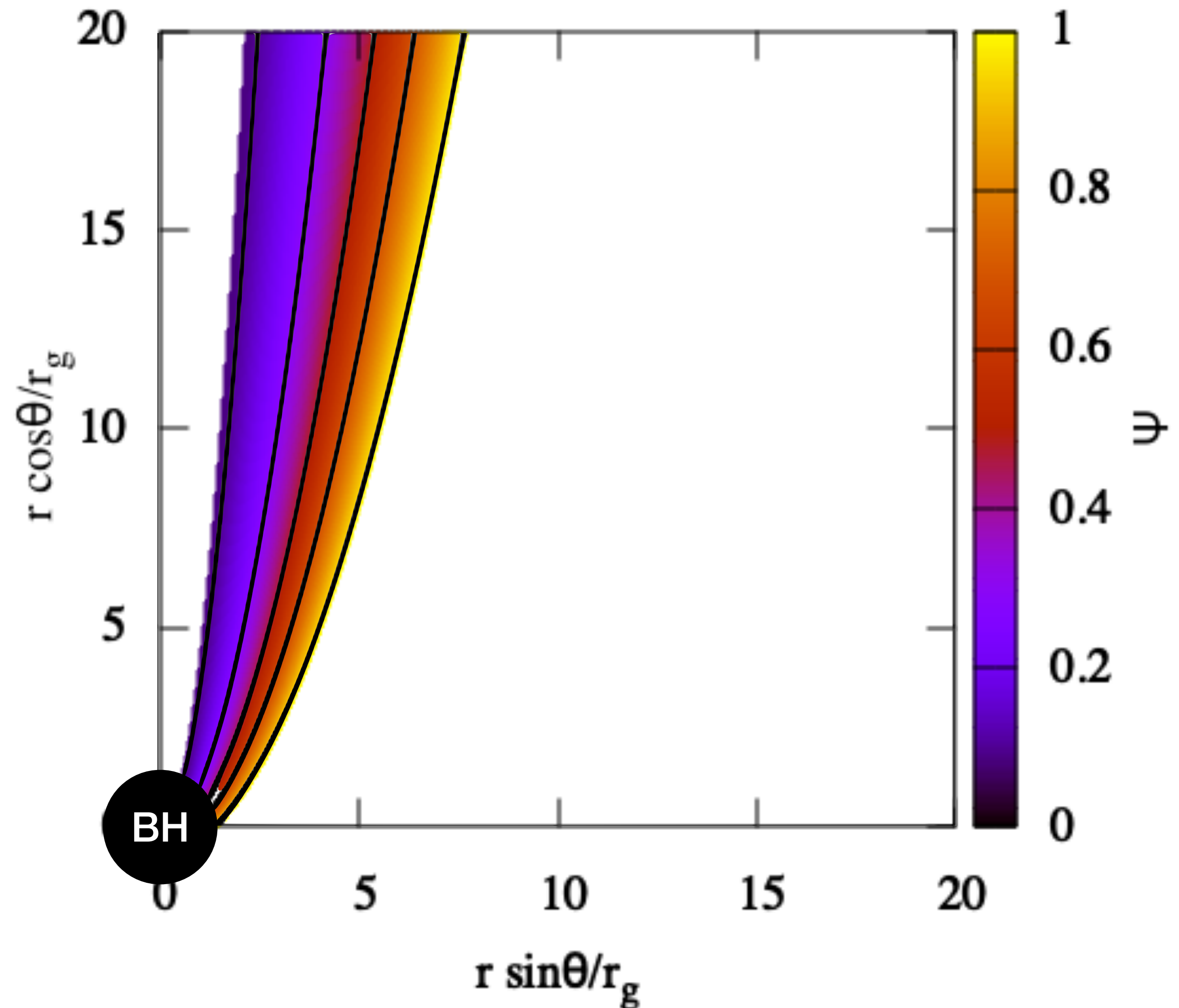
- Boyer-Lindquist coordinate in Kerr spacetime

- steady, axisymmetric $\partial_0 = 0, \partial_3 = 0$

- divide the basic equations into the parallel component to the field line (Bernoulli eq.) and the perpendicular component (Grad-Shafranov eq.)

Field Line Configuration

- flux function:
 $\Psi(r, \theta) = C[(r/r_H)^\nu(1 - \cos \theta) + (1/4)\epsilon r \sin \theta]$
- $\nu = 1$: parabolic field shape
force-free solution
- $\epsilon = 10^{-4}$: MHD deviation
- C : constant. $\Psi(r_H, \pi/2) = 1$
- consistent with results of GRMHD simulations



Integral Constants

- 4 constant quantities along a field line

1. Energy flux per the rest-mass energy : $\hat{E} = -u_0 + \frac{\Omega_F B_3}{4\pi\mu\eta}$

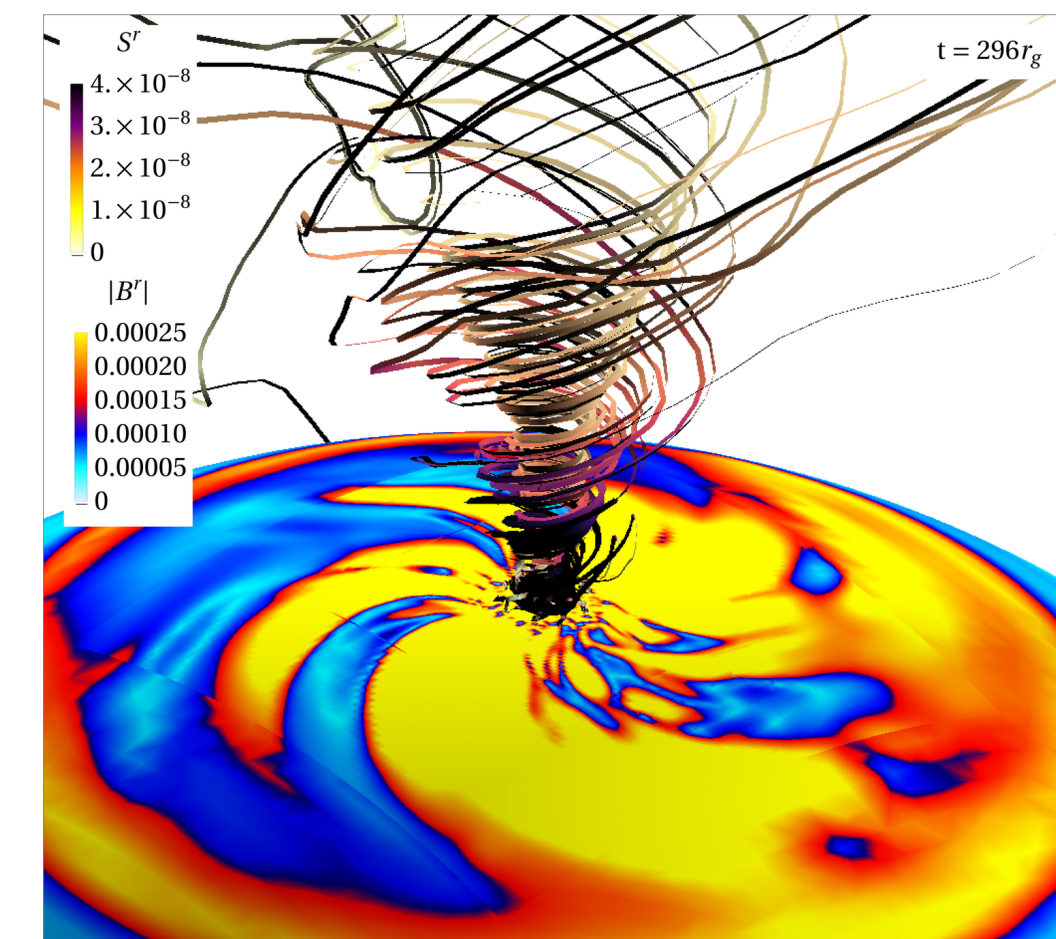
2. Angular momentum flux per the rest-mass energy: $\hat{L} = u_3 + \frac{B_3}{4\pi\mu\eta}$

3. mass flux per magnetic field flux: $\eta = -\frac{nu_1}{B_1}G_t = -\frac{nu_2}{B_2}G_t$ $G_t = g_{00} + \Omega_F g_{03}$

4. “angular velocity” of the field line: $\Omega_F = \frac{F_{01}}{F_{13}} = \frac{F_{02}}{F_{23}}$

$$\mathbf{v}_d = \frac{\mathbf{E} \times \mathbf{B}}{B^2} = R\Omega_F \mathbf{e}_\phi - R\Omega_F \frac{B_\phi}{B^2} \mathbf{B}.$$

If the fluid don't move along the filed line, it rotates with Ω_F .



Mahlmann, Levinson, Aloy 2020

3. Results

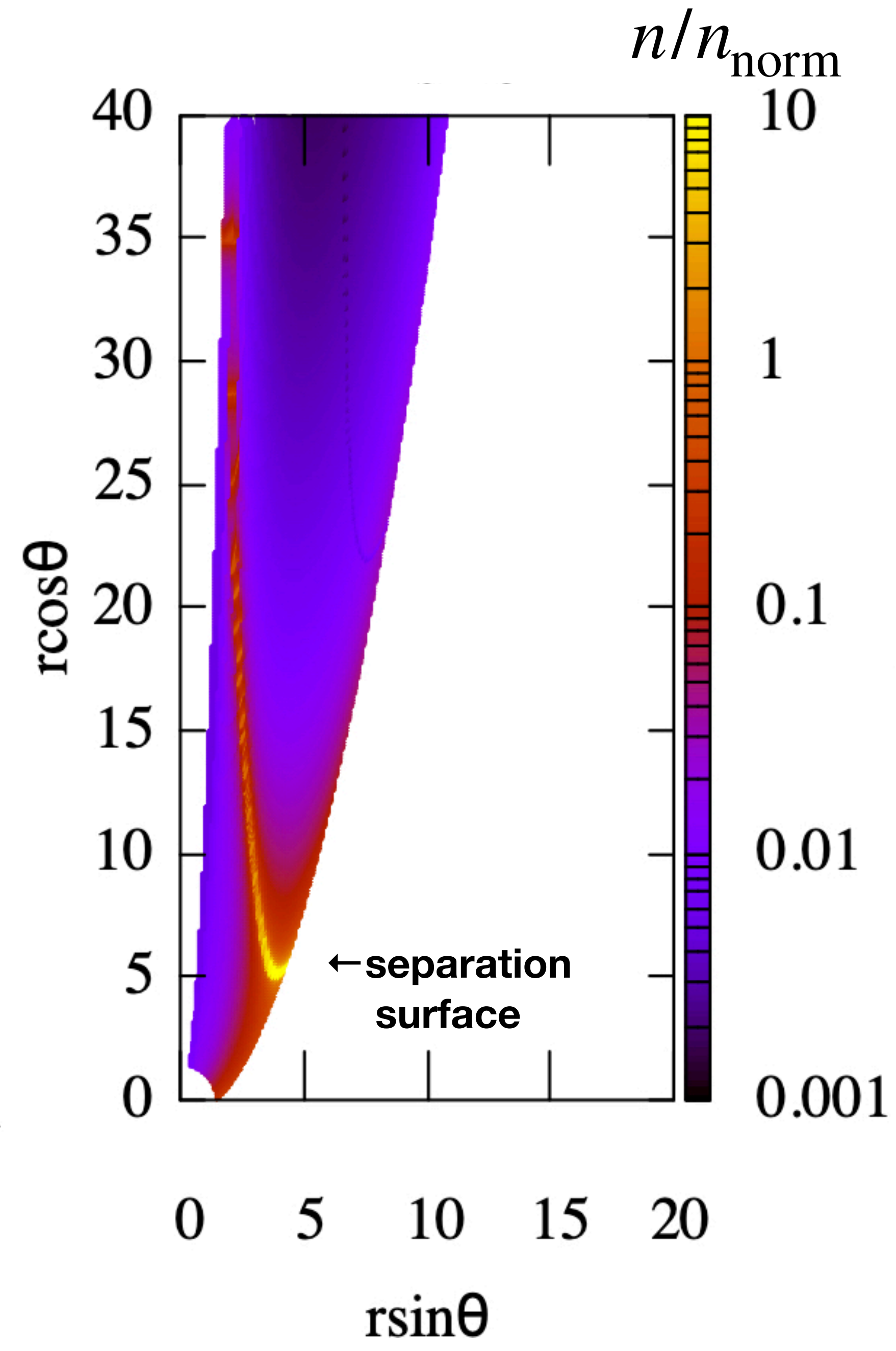
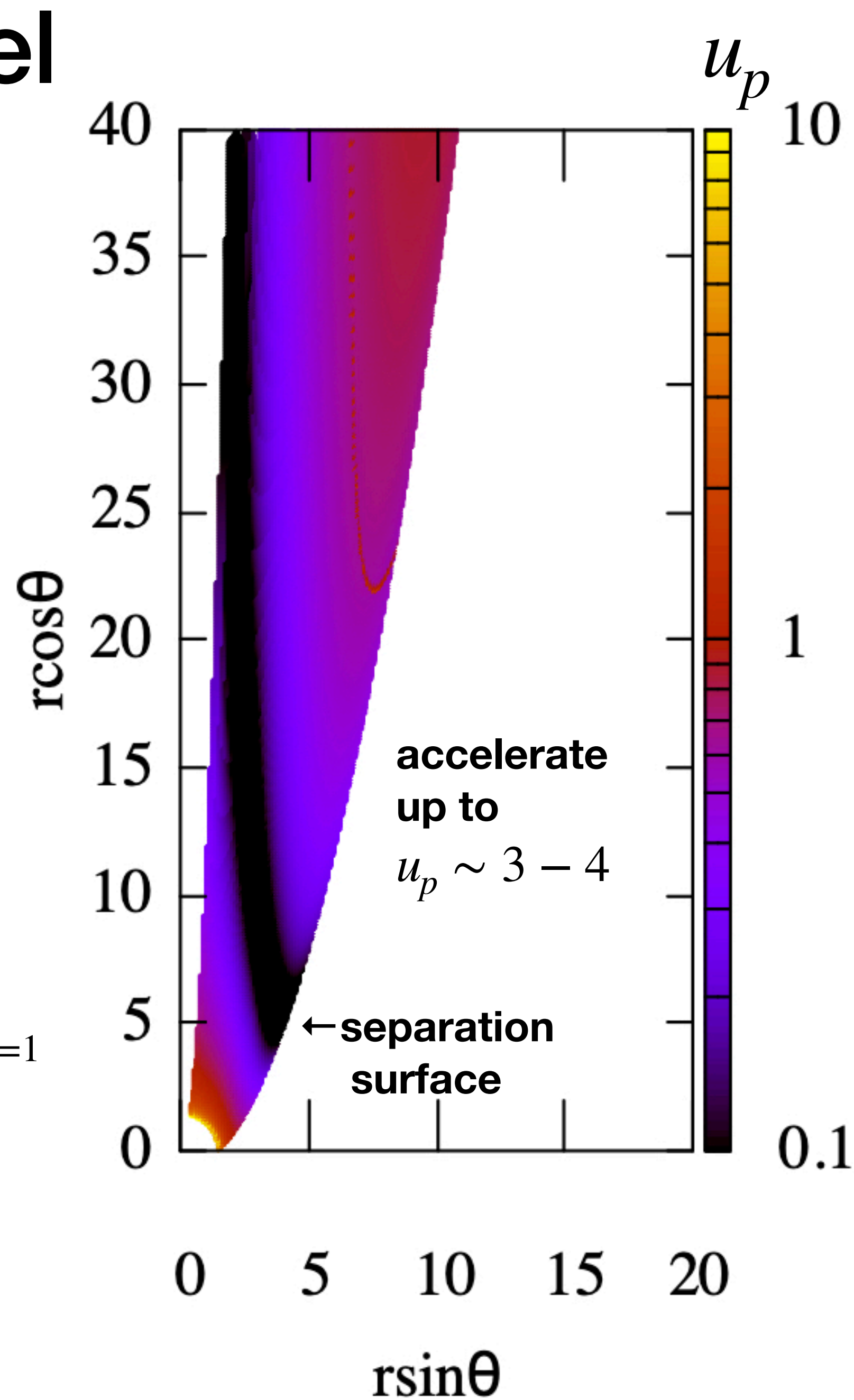
Parabolic Jet Model

- poloidal velocity:

$$u_p^2 = u_1 u^1 + u_2 u^2$$
- flow accelerate from the separation surface

- density normalization:

$$n_{\text{norm}} = \left[\frac{B_1 B^1 + B_2 B^2 + B_3 B^3}{8\pi\mu} \right]_{r=r_{\text{ss}}, \Psi=1}$$



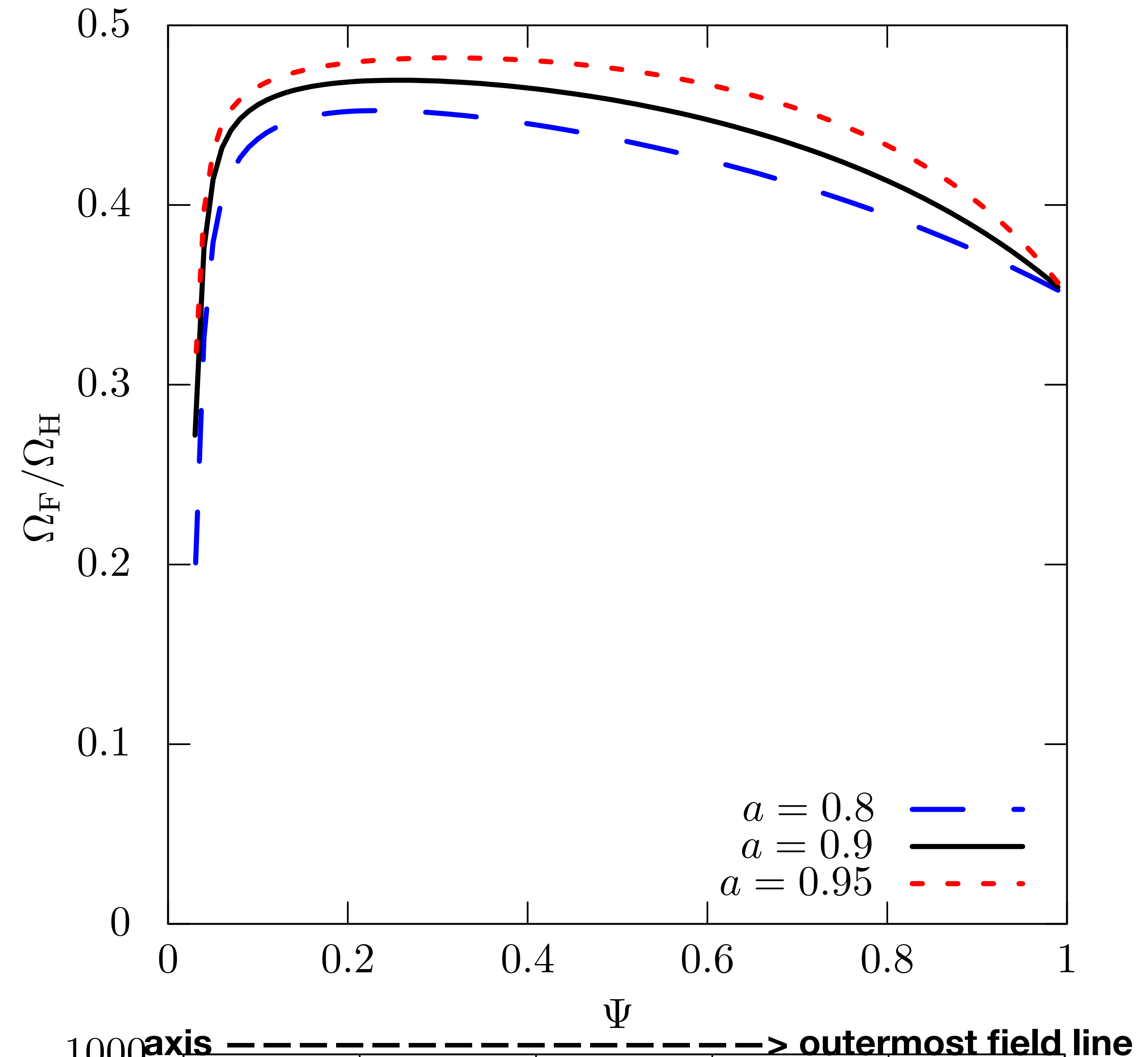
Distribution of Integral Constants and Density

- Ω_F approaches $0.5\Omega_H$ toward the axis like the parabolic force-free analytic solution.

- $$\eta E = -\frac{\rho u_0 u_p G_t}{B_p} + \frac{\Omega_F B_3}{4\pi} \propto \sin^2 \theta$$

dependence of B_3 at the horizon
 → EM dominant jet

- **density: concentrate at $\Psi = 1$**
 - The density contrast becomes higher when the BH spin is larger.



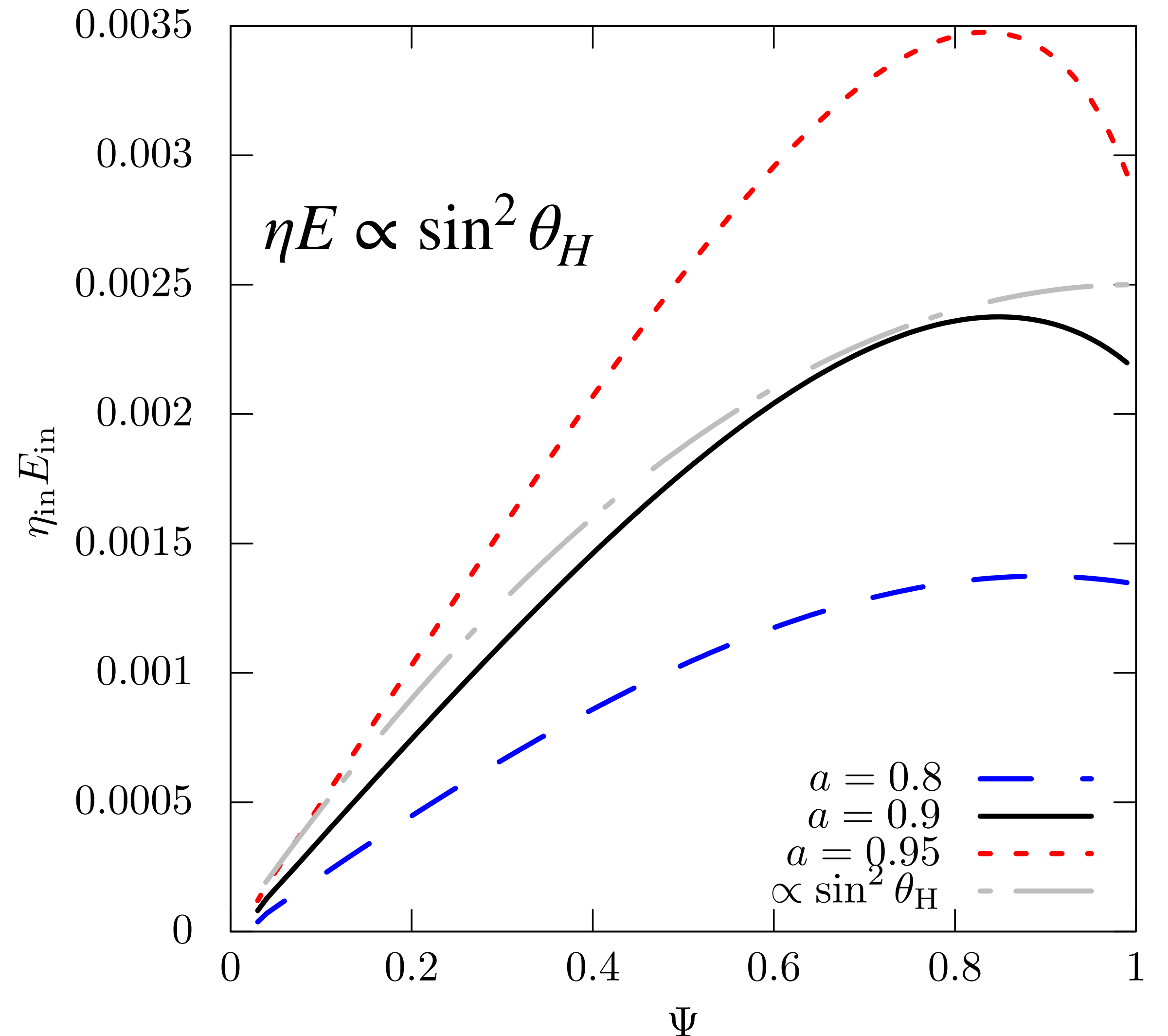
Distribution of Integral Constants and Density

- Ω_F approaches $0.5\Omega_H$ toward the axis like the parabolic force-free analytic solution.

- $$\eta E = -\frac{\rho u_0 u_p G_t}{B_p} + \frac{\Omega_F B_3}{4\pi} \propto \sin^2 \theta_H$$

dependence of B_3 at the horizon
 → EM dominant jet

- **density: concentrate at $\Psi = 1$**
 - The density contrast becomes higher when the BH spin is larger.



axis -----> outermost field line

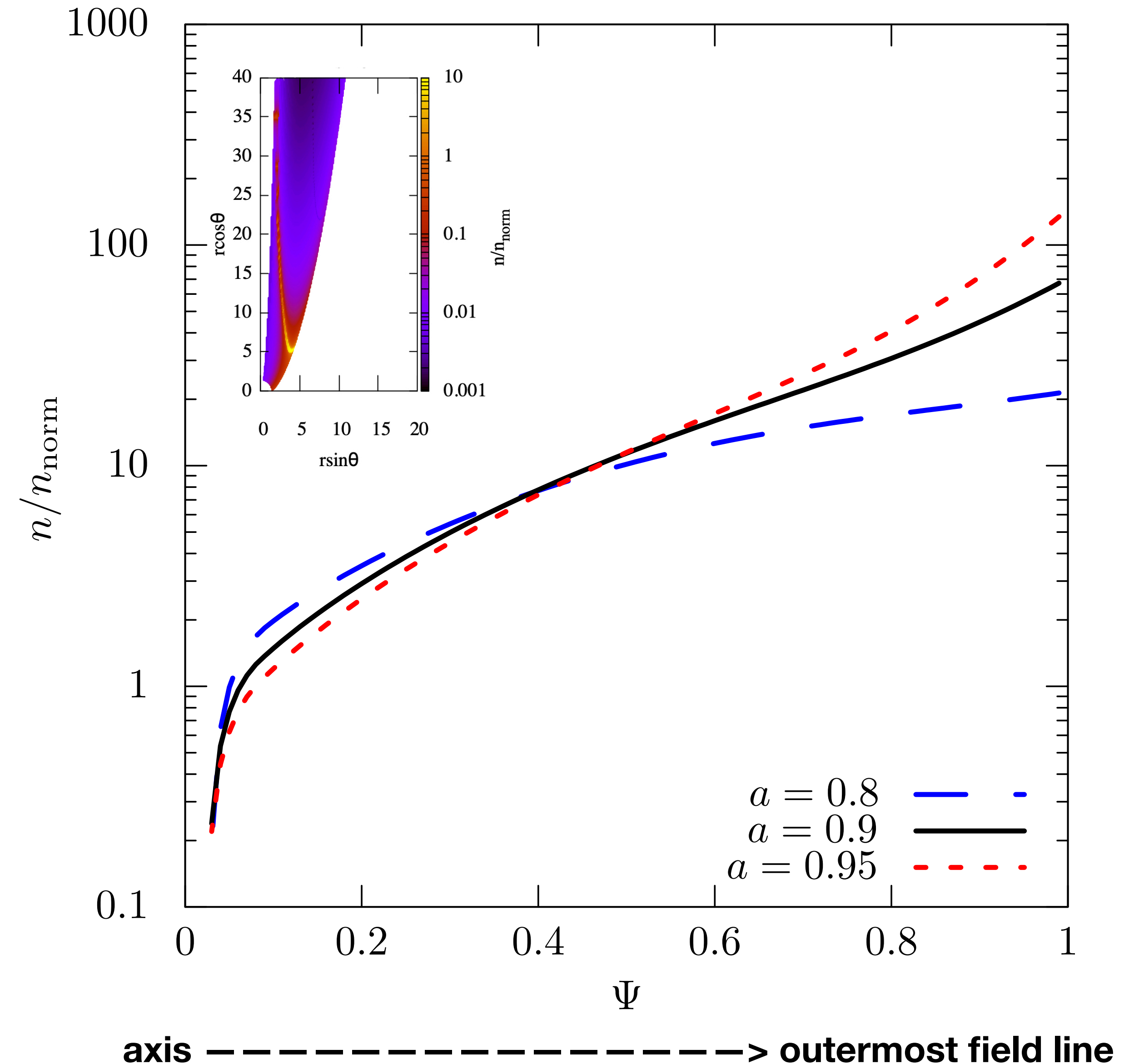
Distribution of Integral Constants and Density

- Ω_F approaches $0.5\Omega_H$ toward the axis like the parabolic force-free analytic solution.

$$\eta E = -\frac{\rho u_0 u_p G_t}{B_p} + \frac{\Omega_F B_3}{4\pi} \propto \sin^2 \theta$$

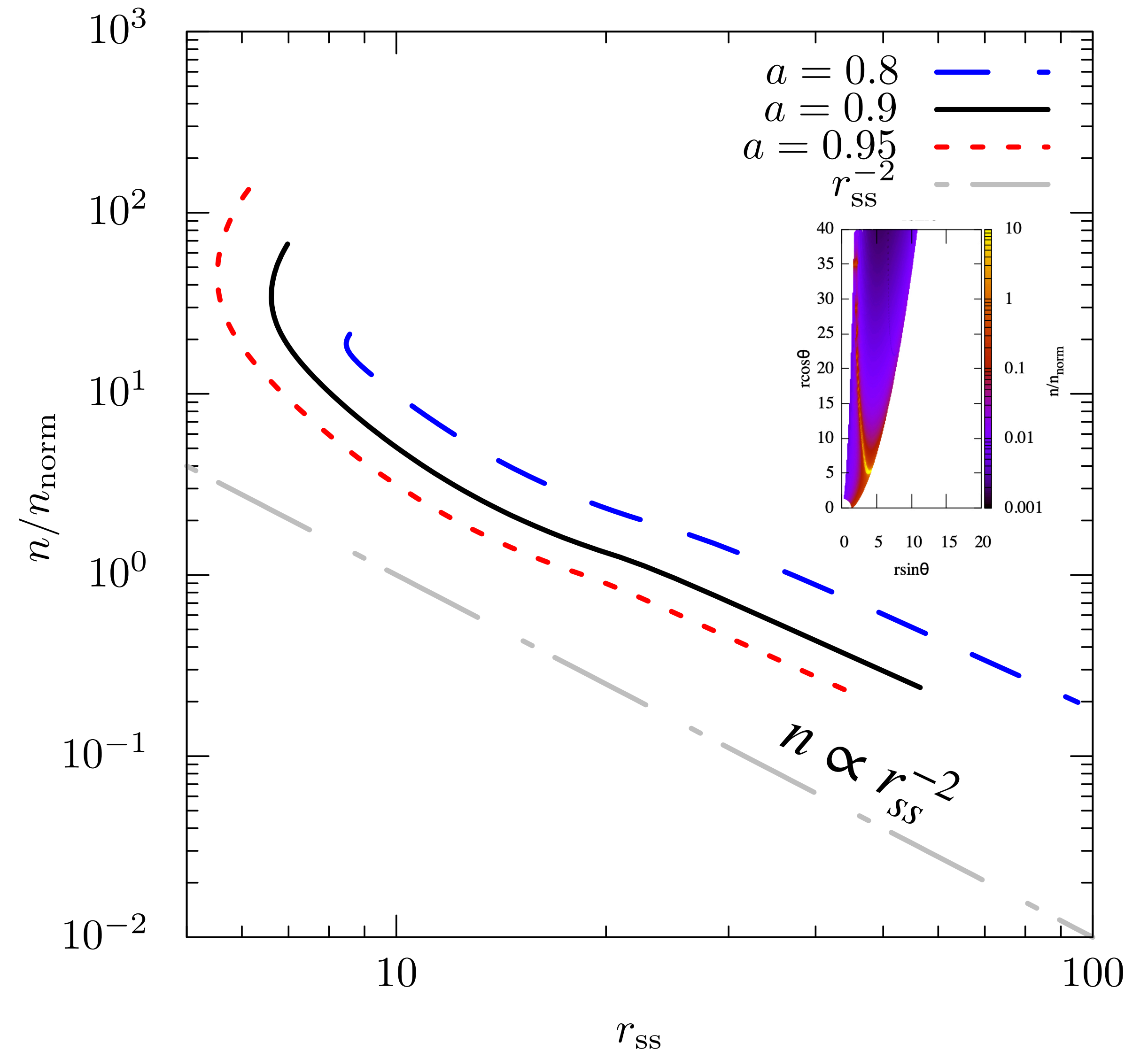
dependence of B_3 at the horizon
 → EM dominant jet

- **density: concentrate at $\Psi = 1$**
 - The density contrast becomes higher when the BH spin is larger.



Density on the Separation Surface

- our result: $n \propto r_{ss}^{-2}$
- **This dependence may change if we change initial velocity distribution $u_{p,ss}(\Psi)$.**
- photon-photon pair creation model
 - $n \propto r^{-6}$ for compact source near BH (Moscibrodzka+ 2011, Wong, Ryan, Gammie 2020)
 - $n \propto r^{-4}$ for distant sources (Kimura & Toma 2020)



Summary

- High resolution VLBI observations have resolved emission structures of jets.
- We have constructed **the steady, axisymmetric GRMHD jet model** which do not suffer from the density floor problem.
- We numerically solve the force-balance between the field lines at the separation surface and analytically solve the distributions of velocity and density along the field lines.
- We determine **the 2D distribution of the EM field, velocity and density in a jet.**
- Our semi-analytic model, **combined with radiative transfer calculations**, may help interpret the high-resolution VLBI observations and understand the origin of jetted matter.

